Science Advances
AAAS

Supplementary Materials for

PD-1/PD-L1 blockade abrogates a dysfunctional innate-adaptive immune axis in critical β-coronavirus disease

Maite Duhalde Vega *et al.*

Corresponding author: Mercedes Segovia, msegovia@pasteur.edu.uy; Marcelo Hill, mhill@pasteur.edu.uy

Sci. Adv. **8**, eabn6545 (2022)
DOI: 10.1126/sciadv.abn6545

This PDF file includes:

Fig. S1

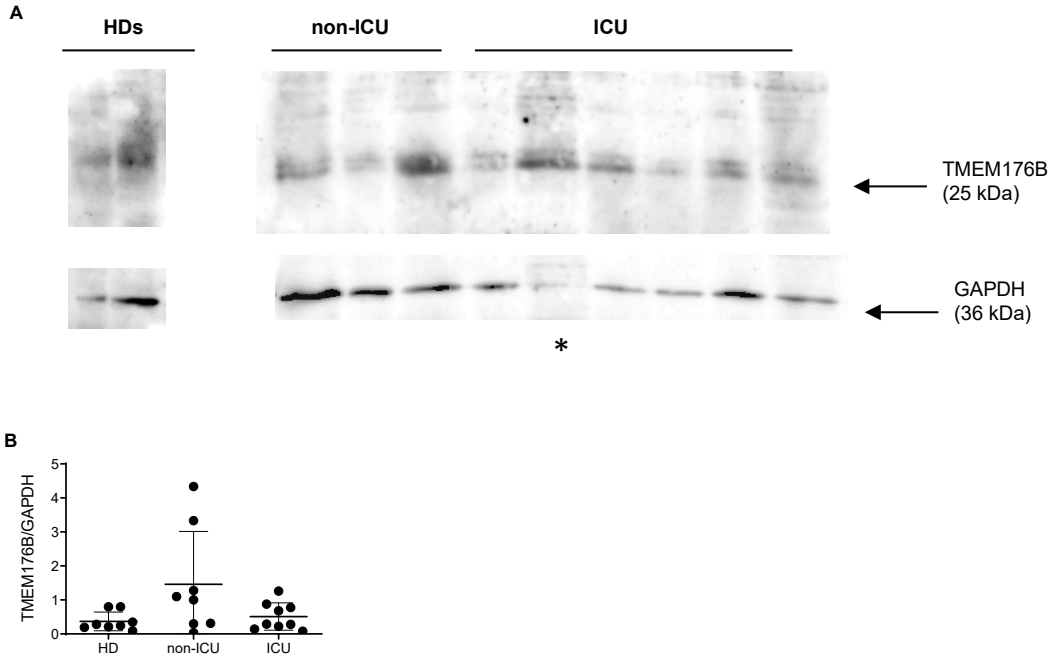

Figure S1. Western blot study of TMEM176B/GAPDH ratios in peripheral blood CD14^{+} monocytes from healthy donors (HDs), non-ICU and ICU patients.
(A) Representative western blot. * Sample not considered for the analysis due to low GAPDH.
(B) Graphic depicting all the studied patients.

Fig. S2

A

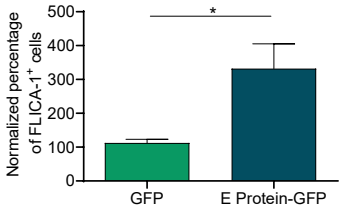

B

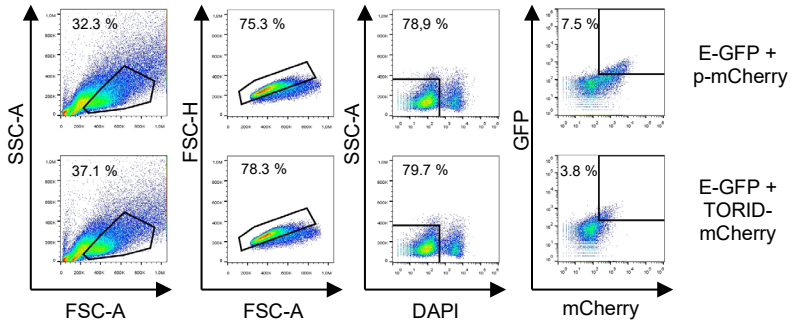

Figure S2. Study on inflammasome activation in human THP-1 monocytes transfected with plasmids coding for GFP, E Protein-GFP, mcherry and TMEM176Bmcherry.

(A) Study of FLICA-1^{+} cells. A pool of two experiments is shown. * p< 0.05. One sample *t* test.
(B) Gating strategy. One experiment representative of three is shown.

Fig. S3

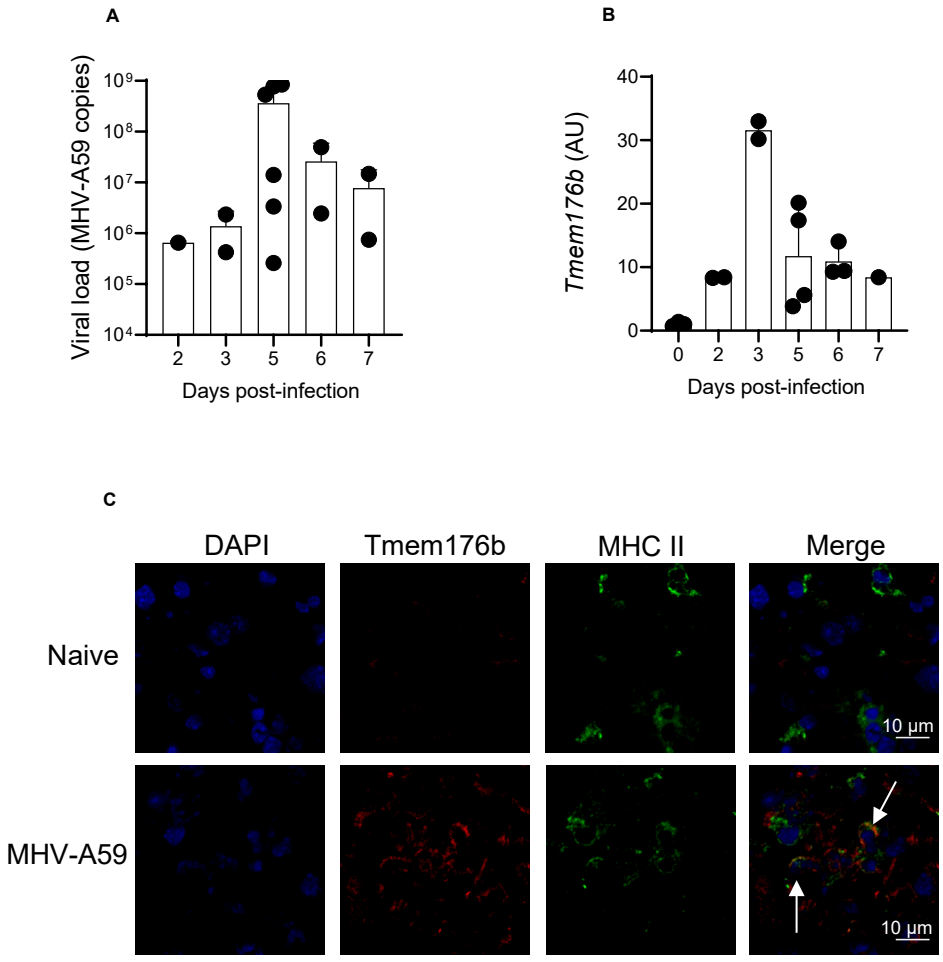

Figure S3. Viral load and Tmem176b expression in the liver of MHV-A59-infected mice.
(A) Viral load was analyzed by RT-qPCR in the liver of WT mice at different days post-infection.
(B) *Tmem176b* expression was studied by RT-qPCR in the liver of WT mice at different days post-infection.
(C) Mouse liver cryosections from MHV-A59-infected or naive animals were stained with anti MHC class II and TMEM176B antibodies, then the nucleus was stained with DAPI and analyzed by confocal microscopy. Animals were sacrificed at 5 dpi. The arrows show MHC class II+ Tmem176b+ cells. Images are representative of 4 naive and 4 infected animals.

.

Fig. S4

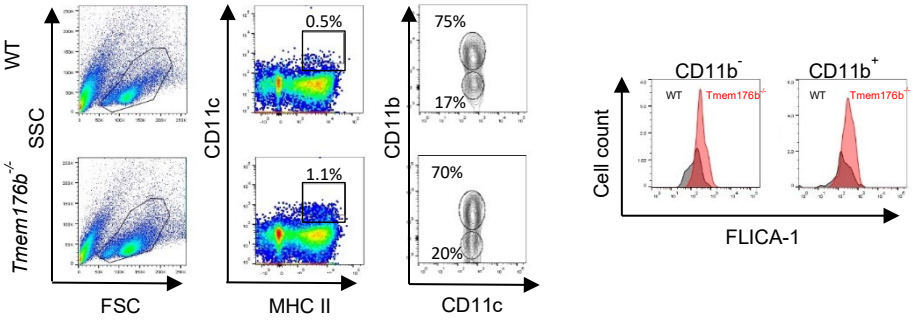

Figure S4. Gating strategy to study conventional DCs infiltrating the liver of WT and Tmem176b$^{-/-}$ mice.

Analysis of FLICA-1 staining shown in Fig. 1 K-L was done in CD11b^{-} and CD11b^{+} conventional DCs as defined here. One experiment representative of three is shown.

Fig. S5

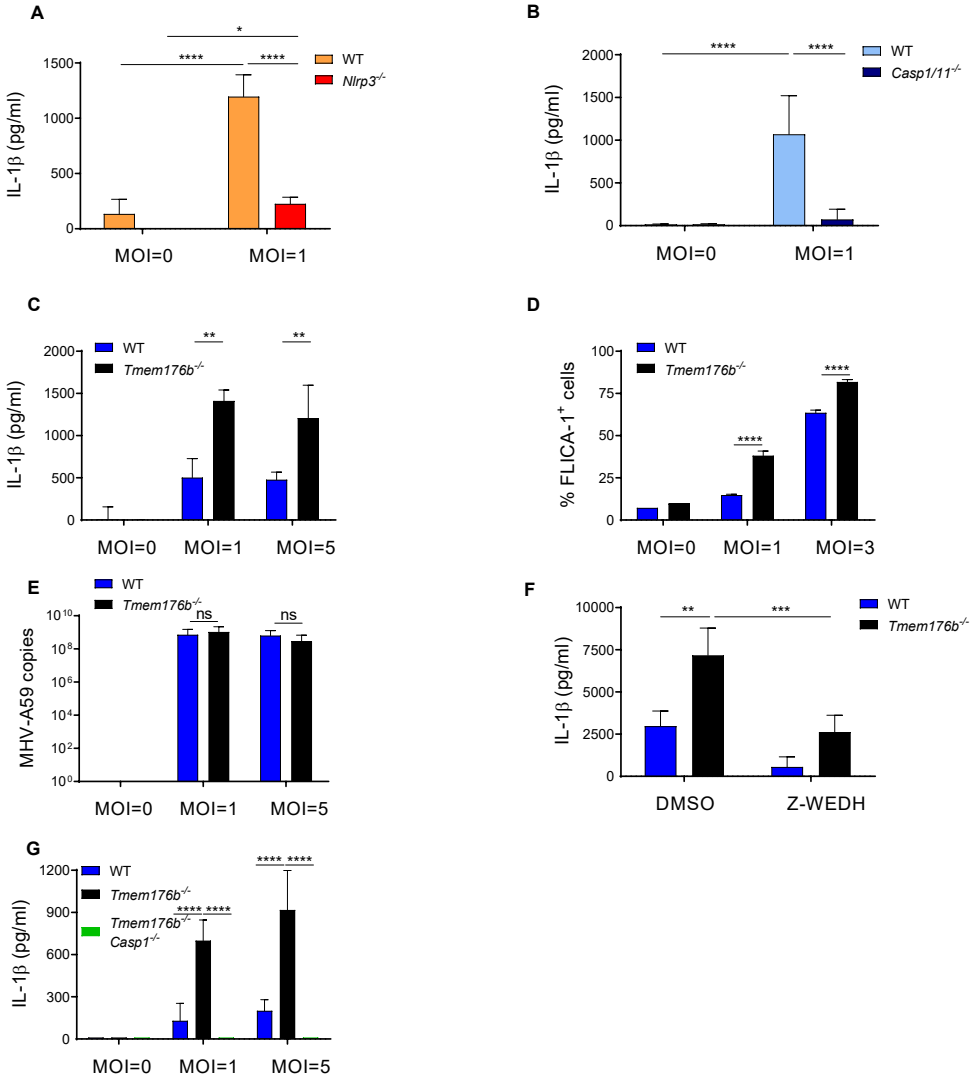

Figure S5. Tmem176b controls MHV-A59-triggered NLRP3 inflammasomes in bone marrow-derived dendritic cells (BMDCs)

(A) WT and *Nlrp3*$^{-/-}$ BMDCs were left untreated or infected with MHV-A59. IL-1β was assessed by ELISA in the culture supernatant. One experiment representative of three is shown. * p<0.05; **** p<0.0001. Two-way ANOVA test.

(B) WT and *Casp1/11*$^{-/-}$ BMDCs (both in C57BL/6JN background) were infected with MHV-A59 and IL-1β was assessed by ELISA in the culture supernatant. One experiment representative of three is shown. ****p<0.0001. Two-way ANOVA test.

(C) WT (issued from littermate controls) and *Tmem176b*$^{-/-}$ BMDCs were infected with MHV-A59 at the indicated multiplicities of infection (MOIs). IL-1β was assessed by ELISA in the culture supernatant. One experiment representative of four is shown. ** p<0.01. Two-way ANOVA test.

(D) Caspase-1 activity was studied by staining WT and *Tmem176b*$^{-/-}$ BMDCs with FLICA-1 followed by flow cytometry analysis. One experiment representative of three is shown. **** p<0.0001. Two-way ANOVA test.

(E) WT and *Tmem176b*$^{-/-}$ BMDCs were infected with MHV-A59 at the indicated MOIs. MHV-A59 copies were assessed by RT-qPCR. A pool of two experiments is shown. ns: not significant. Two-way ANOVA test.

(F) WT and *Tmem176b*$^{-/-}$ BMDCs were infected with MHV-A59 in the presence of DMSO (vehicle control) or the Caspase-1 inhibitor Z-WEDH. IL-1β was assessed by ELISA in the culture supernatant. One experiment representative of three is shown. ** p<0.01; *** p<0.001. Two-way ANOVA test.

(G) WT, *Tmem176b*$^{-/-}$ and *Tmem176b*$^{-/-}$ *Casp1*$^{-/-}$ BMDCs were infected with MHV-A59 at the indicated MOIs. IL-1β was assessed by ELISA in the culture supernatant. One experiment representative of three is shown. **** p<0.0001. Two-way ANOVA test.

Fig. S6

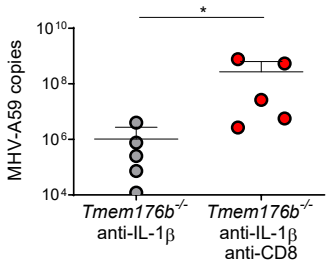

Figure S6. Depletion of the CD8 compartment increases viral load in Tmem176b$^{-/-}$ mice treated with anti-IL-1β antibodies.

Tmem176b$^{-/-}$ mice were infected with MHV-A59 at day 0 through i.p. injection. One µg anti-IL-1β was injected i.p every 5 days since day -2. One hundred µg anti-CD8 antibody was injected i.p every 3 days since day -2. Viral load was assessed by RT-PCR in livers at 5 dpi. Mann-Whitney test. * $p < 0.05$.

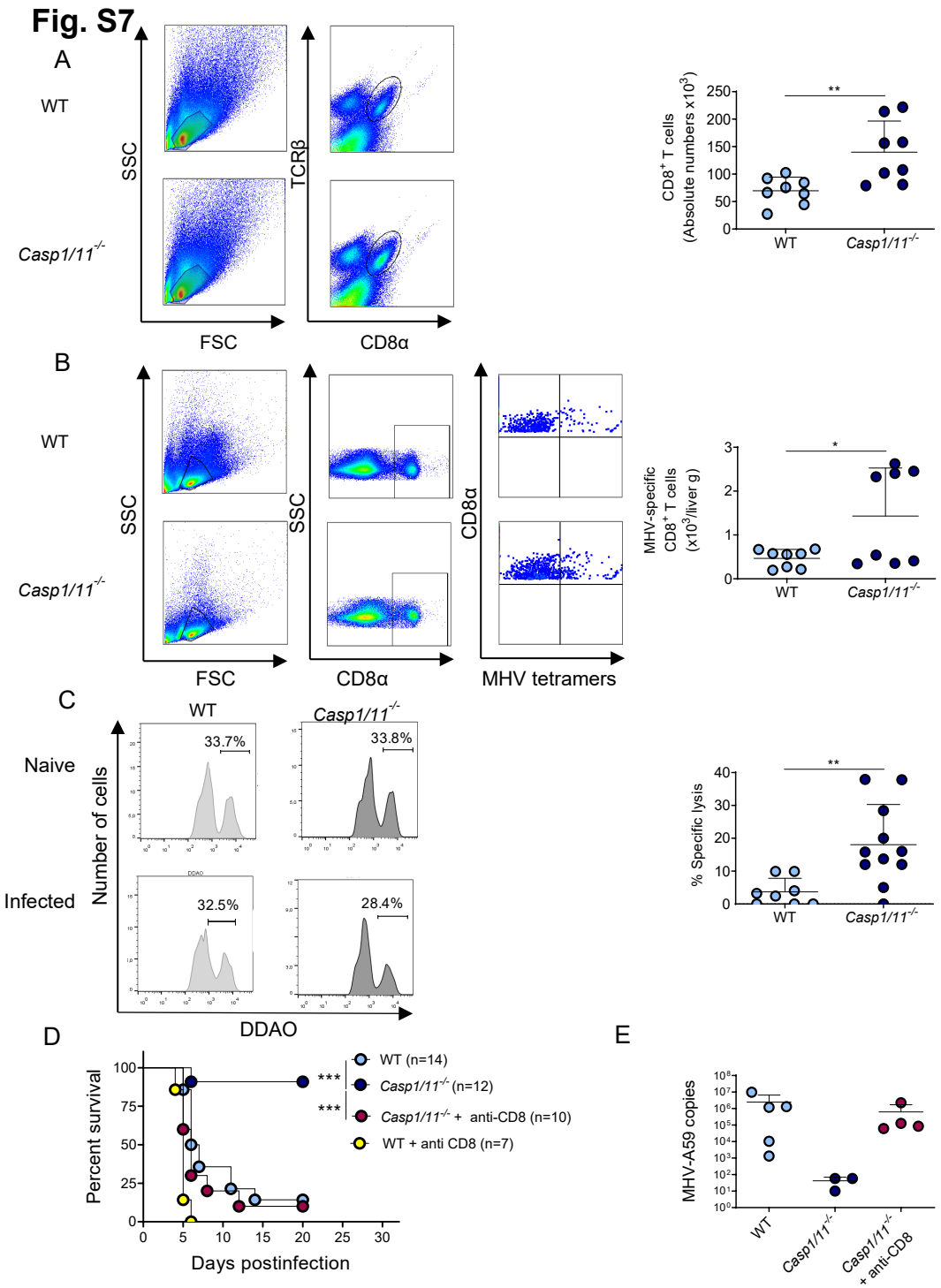

Figure S7. Casp1/11 deficiency is associated with reinforced CD8+ T cell responses and improved outcome of MHV-A59 infection.

(A) WT and *Casp1/11*$^{-/-}$ mice were infected with MHV-A59 (1200 PFU). Total CD8^{+} T cells were studied by flow cytometry in the spleen. The left panel shows representative dot plots whereas the right graphic shows the absolute number of CD8^{+} T cells for 8 WT and 8 *Casp1/11*$^{-/-}$ mice. ** p<0.01. Student's *t* test.

(B) MHV-specific CD8^{+} T cells in the spleen were studied in the animals used in A. * p<0.05. Student's *t* test.

(C) *In vivo* MHV-sp cytotoxic (CTL) activity assay was performed on 8 WT and 11 *Casp1/11*$^{-/-}$ infected mice at 5 dpi. Representative histograms are shown in the left panel. The percentage of specific lysis was calculated with the formula showed in the materials and methods section. ** p<0.01. Student's *t* test.

(D) Mouse survival was studied in MHV-A59-infected WT (C57BL/6JN) and *Casp1/11*$^{-/-}$ animals treated with depleting anti-CD8 antibody. One hundred µg anti-CD8 antibody was injected i.p every 3 days since day -2. CD8 depletion was confirmed by flow cytometry. *** p< 0,001. Log-rank (Mantel-Cox) test.

(E) Viral load was analyzed by RT-qPCR in the liver of 5 WT and 3 *Casp1/11*$^{-/-}$ as well as 4 *Casp1/11*$^{-/-}$ animals treated with depleting anti-CD8 antibody. ns One-way ANOVA test.

Fig. S8

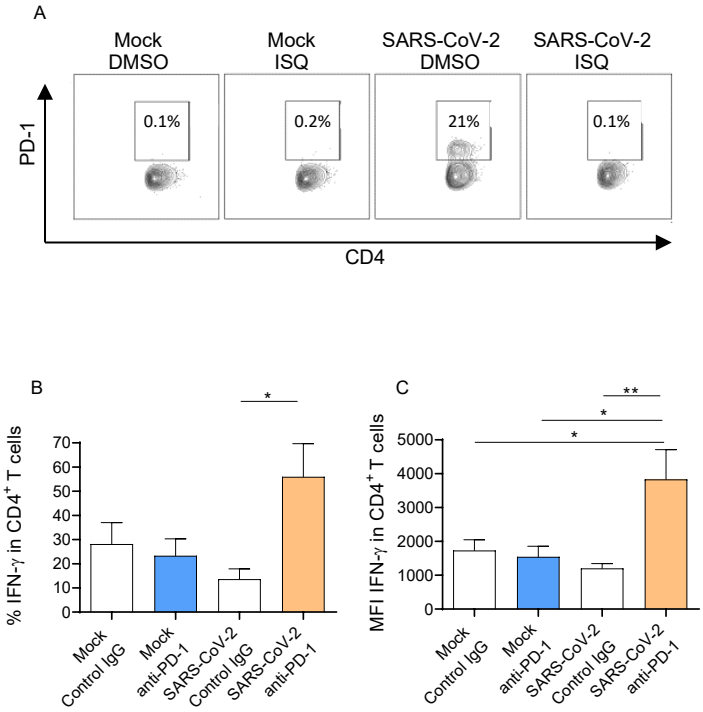

Figure S8. Impact of cell culture media from infected monocytes on the functionality of alloreactive CD4+ T cells

(A) Study of PD-1 expression by $CD4^+$ $TCR\text{-}\beta^+$ cells co-cultured with allogeneic monocytes ± cell culture media (CCM) from SARS-CoV-2-infected monocytes ± 5μM ISQ. One experiment representative of three is shown.

(B-C) Flow cytometry study of IFN-γ expression by $CD4^+$ T cells co-cultured with allogeneic monocytes ± CCM from uninfected monocytes (Mock) or SARS-CoV-2-infected cells ± anti-PD-1 or control antibody (20 μg/ml). The percentage of IFN-γ^+ cells is shown in B and the mean fluorescence intensity (MFI) of positive cells in C. The graphics show one expreriment representative of three. * $p<0.05$; ** $p < 0.01$. One-way ANOVA test.

Fig. S9

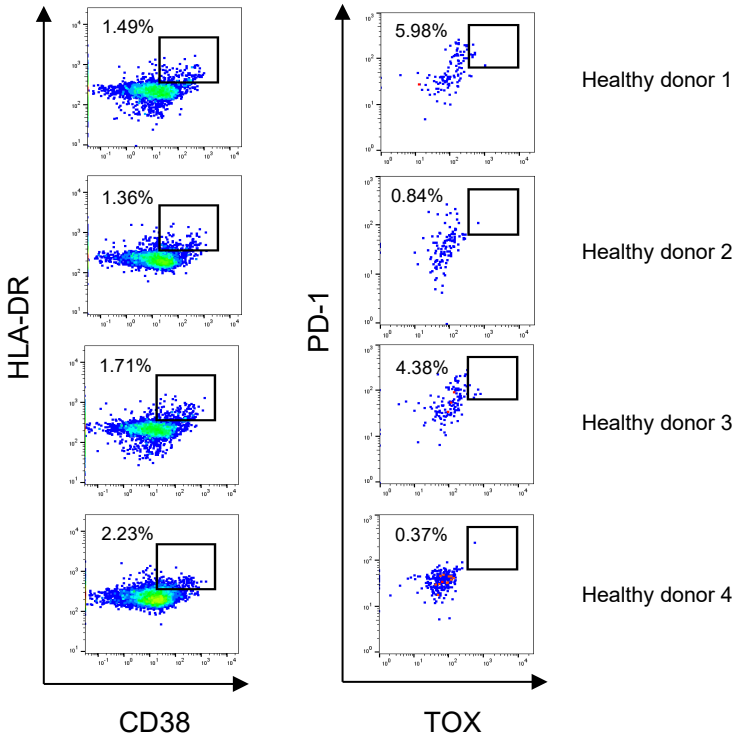

Figure S9. Flow cytometry study of HLA-DR/CD38 within peripheral blood CD8$^+$ T cells and TOX/PD-1 within HLA-DR$^+$ CD38$^+$ CD8$^+$ T cells from healthy donors.

Fig. S10

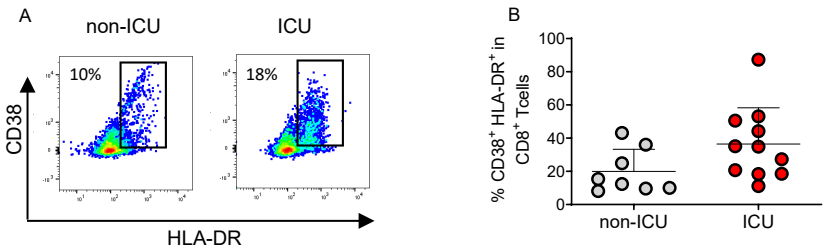

Figure S10. Flow cytometry study of HLA-DR/CD38 in CD8$^+$ T cells from non-UCI and UCI patients.
(A) Representative dot plots.

(B) The graphic shows the individual percentages of CD38$^+$ HLA-DR$^+$ cells within CD8$^+$ TCR-β$^+$ for each studied patient. p= 0.07. Student's *t* test.

Fig. S11

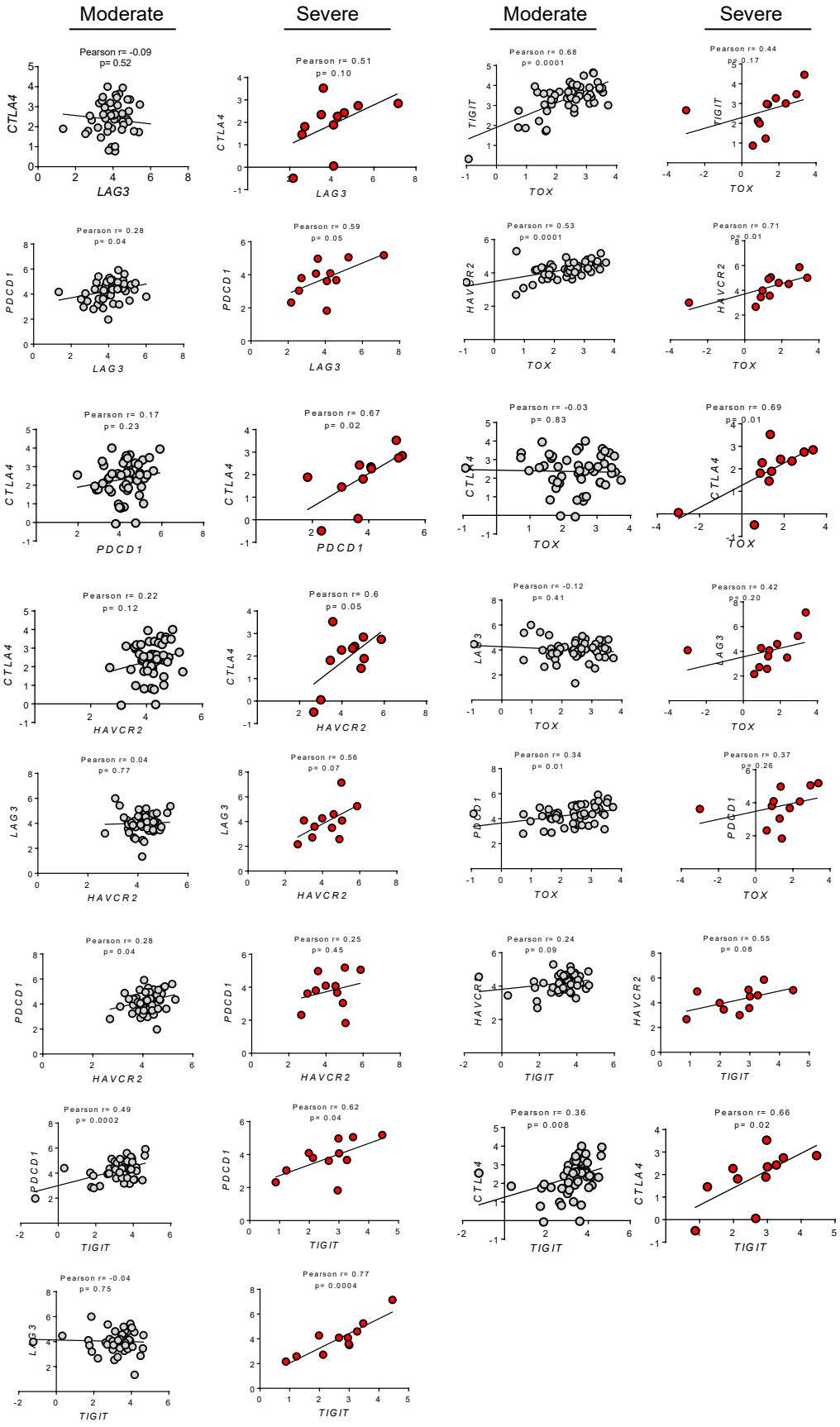

Figure S11. Correlation of the indicated genes in moderate and severe COVID-19 patients from McClain et al. (46).

Fig. S12

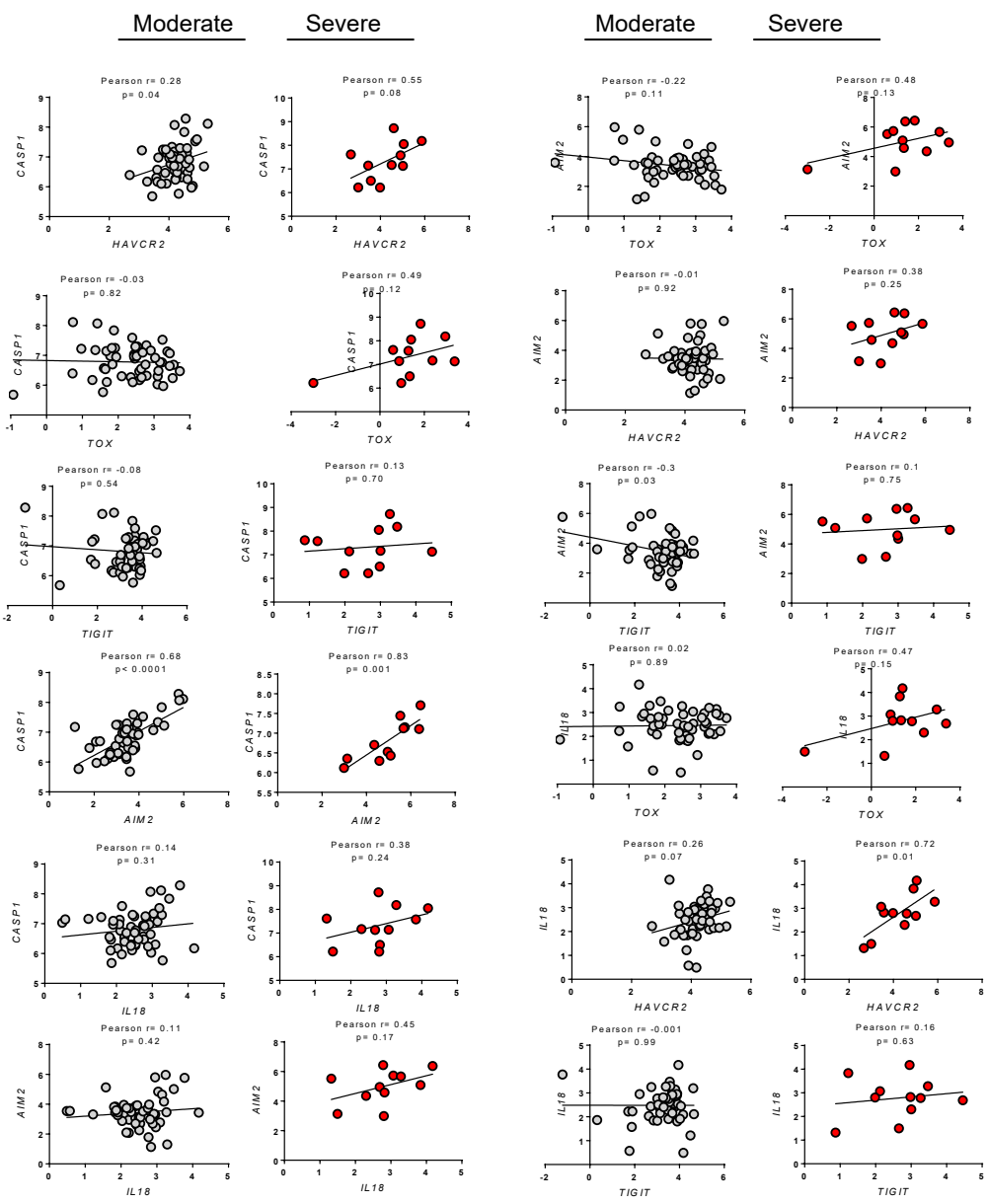

Figure S12. Correlation of the indicated genes in moderate and severe COVID-19 patients from McClain et al. (46).

Fig. S13

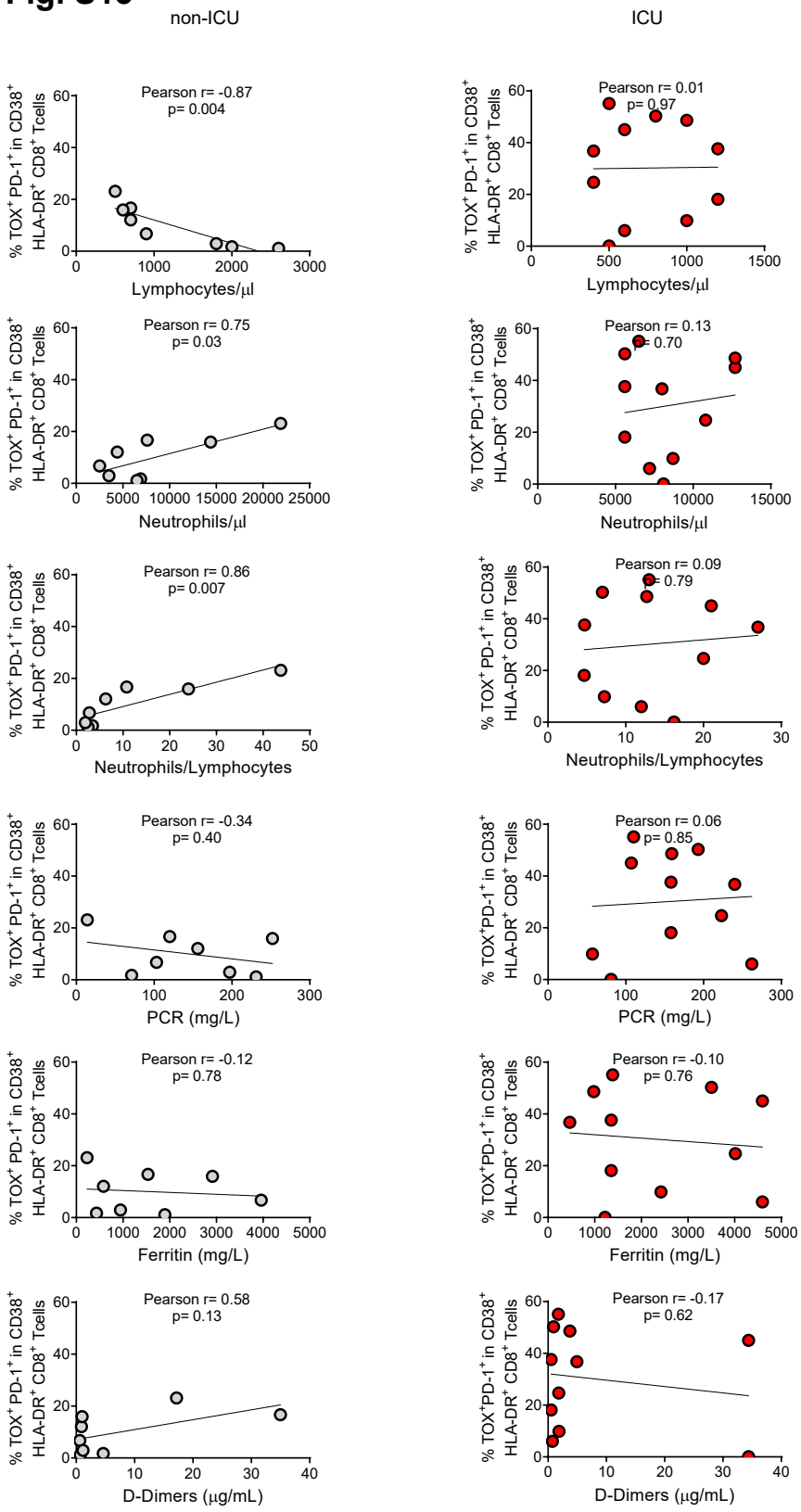

Figure S13. Correlation of the indicated parameters in non-ICU and ICU patients.

Fig. S14

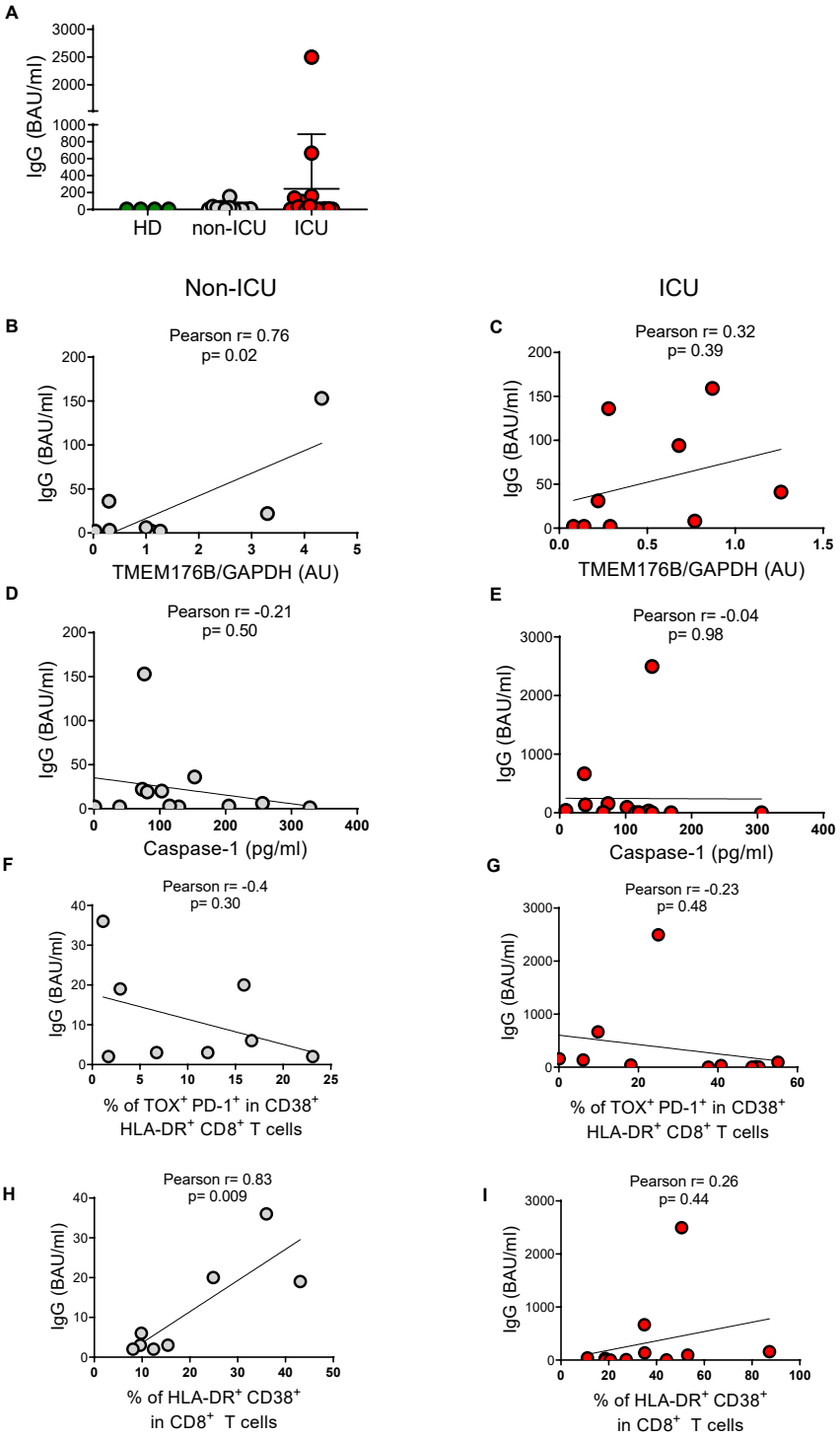

Figure S14. Correlation of anti-SARS-CoV-2 spike IgG with the indicated parameters.
Plasmatic anti-SARS-CoV-2 spike IgG were measured by ELISA.
(A) Anti-SARS-CoV-2 spike IgG levels in healthy donors (HDs), non-ICU and ICU patients.
(B, D, F and H) non-ICU patients.
(C, E, G and I) ICU patients.
(B-C) TMEM176B/GAPDH ratio was determined by western blot in samples peripheral blood $CD14^+$ monocytes and expressed in arbitrary units (AU).
(D-E) Active Caspase-1 was assessed by ELISA in plasma
(F-G) TOX^+ $PD\text{-}1^+$ in $HLA\text{-}DR^+$ $CD38^+$ $CD8^+$ T cells from peripheral blood were studied by flow cytometry.
(H-I) $HLA\text{-}DR^+$ $CD38^+$ $CD8^+$ T cells from peripheral blood were studied by flow cytometry.

Fig. S15

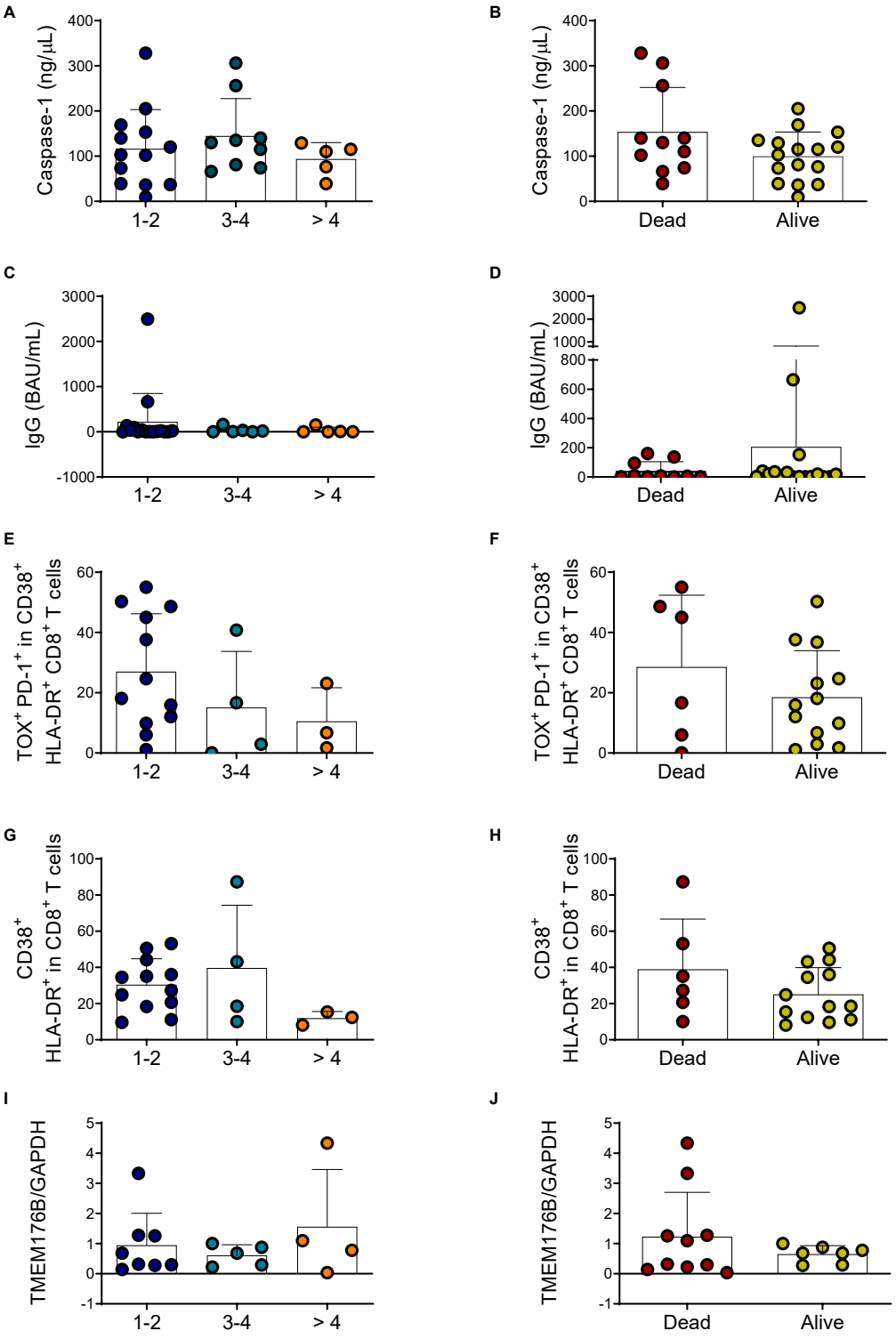

Figure S15. Study of Charlson comorbidity index (A, C, E, G and I) and mortality (B, D, F, H and J) versus the indicated parameters.

(A-B) Active Caspase-1 was assessed by ELISA in plasma

(C-D) Anti-SARS-CoV-2 spike IgG was determined by ELISA in plasma.

(E-F) TOX^+ $PD\text{-}1^+$ in $HLA\text{-}DR^+$ $CD38^+$ $CD8^+$ T cells from peripheral blood were studied by flow cytometry.

(G-H) $HLA\text{-}DR^+$ $CD38^+$ $CD8^+$ T cells from peripheral blood were studied by flow cytometry.

(I-J) TMEM176B/GAPDH ratio was determined by western blot in samples peripheral blood $CD14^+$ monocytes and expressed in arbitrary units (AU).

Fig. S16

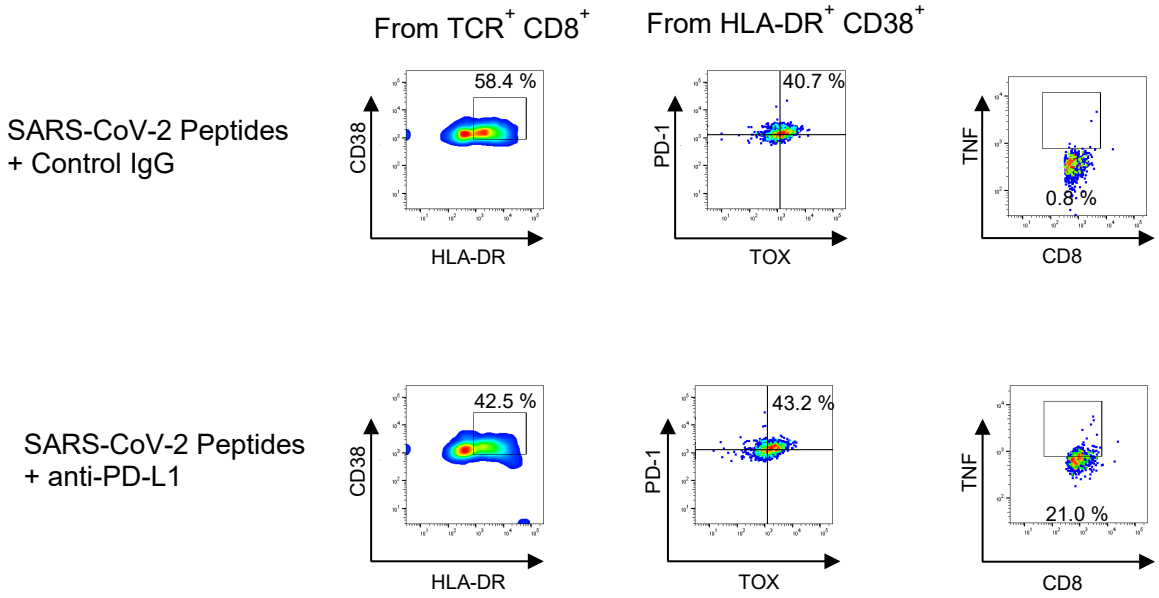

Figure S16. PD-L1 blockade triggers TNF production by CD38+ HLA-DR+ PD-1+ TOX+ CD8+ T cells treated with SARS-CoV-2 peptides.

PBMCs from three lymphopenic critical patients were studied. Cells were incubated for 24 h with 20 µg/ml control IgG (human IgG1) or anti-PD-L1 antibody. Then, 6 nmol SARS-CoV-2 peptides were added to the culture for 6 h. Representative dot plots are shown.

Fig. S17

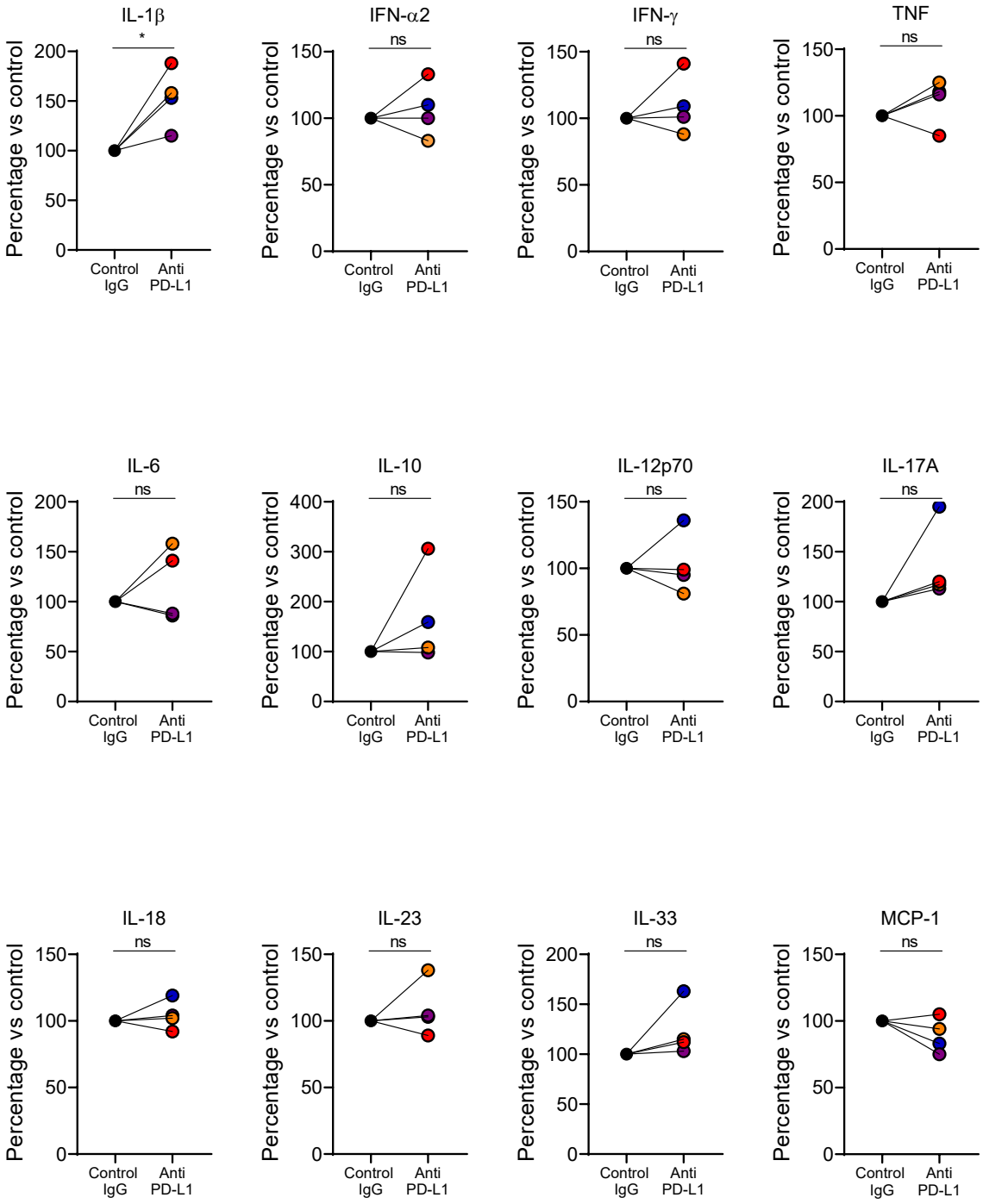

Figure S17. Study of cytokines secreted in the culture supernatant of PBMCs form ICU patients.
Supernatants of PBMCs cultures used in Figure 4G-H were assessed for an array of 12 cytokines. Cells were incubated for 24 h with 20 µg/ml control IgG (human IgG1) or anti-PD-L1 antibody. Then, 6 nmol SARS-CoV-2 peptides were added to the culture for 6 h. Cytokines were quantified by flow cytometry using a bead-cased multiplex kit. Absolute values were standardized in relationship to the control condition (100%). One sample *t* test. ns= not significant; * p< 0.05.

Characteristic	
No.	30
Age, median (IQR), years	65.5 (53.0 – 76.0)
Male	22/30 (73.3 %)
Female	8/30 (26.7 %)
Length of hospital stay, median (IQR), days	18 (10 – 33)
WHO-CPS score, median (IQR)	8 (5 – 10)
Charlson co-morbidity index, median (IQR)	2 (1 – 3)
ICU	19/30 (63.3 %)
non-ICU	11/30 (36.7 %)
Temperature, median (IQR), ºC	37.8 (37.0 – 38.0)
Respiratory rate, median (IQR), bpm	25.5 (24.0 – 28.0)
SpO_2, median (IQR), %	88.0 (86.0 – 89.0)
Co-existing conditions	10/30 (33.3 %)
Dementia	3/30 (10.0 %)
Diabetes mellitus	3/30 (10.0 %)
Chronic obstructive pulmonary disease	3/30 (10.0 %)
Congestive heart failure	1/30 (3.3 %)
Connective tissue diseases	1/30 (3.3 %)
Ischemic cardiomyopathy	1/30 (3.3 %)
Smoking	
No	26/30 (86.7 %)
Current	1/30 (3.3 %)
Former	3/30 (10.0 %)
Laboratory values, median (IQR)	
CRP, mg/L	158.0 (107.8 – 196.0)
D-Dimer, µg/mL	1.8 (0.7 – 4.2)
Neutrophile count, cells/µL	6100 (4500 – 9125)
Lymphocyte count, cells/µL	850 (500 -1200)
Lymphocytes to Neutrophiles ratio	0.14 (0.08 – 0.29)
Hemoglobin, g/dL	13.8 (13.4 – 15.7)
Platelet count, number $x10^3$/µL	211.0 (176.0 – 262.5)
AST, IU/L	59.0 (44.0 – 76.0)
ALT, IU/L	46.0 (39.0 – 74.3)
Albumin, g/dL	3.7 (3.5 – 4.1)
Creatinine, mg/dL	1.1 (0.9 – 1.4)
Azotemia, mg/dL	48.0 (35.0 – 65.0)
Ferritin, mg/L	1354.0 (581.0 – 2545.5)
LDH, IU/L	467.5 (339.0 – 683.0)
Number of deaths	12/30 (40.0 %)

Table S1. Characteristics of the studied patients.

IQR: Interquartile range